

Motion Planning for Multiple Mobile Manipulators*

Jaydev Desai, Chau-Chang Wang, Miloš Žefran and Vijay Kumar

General Robotics and Active Sensory Perception (GRASP) Laboratory, University of Pennsylvania
3401 Walnut Street, Room 301C, Philadelphia, PA 19104-6228

Abstract

We address the motion planning for “fixtureless” material-handling with multiple manipulators on non-holonomic carts. The mobile manipulators possess the ability to manipulate and transport objects while holding them in a stable grasp. We present a general approach that allows generation of optimal trajectories and actuator inputs for any given maneuver. Constraints such as limitations on the turning radii of the mobile manipulators or bounds on their separation can be easily incorporated into the planning scheme. Numerical solutions for several maneuvers including abrupt turns, parallel parking in cluttered environments and changes in formation are computed. Finally, we present experimental results with two mobile manipulators.

1 Introduction

A mobile, multi-robot system can interface between fixed workcells and play the role of the human operator by off-loading components from special-purpose material-handling equipment, loading workpieces on fixtures for machines/work cells, and fetching appropriate tools. Multiple mobile robots could be used where the payloads cannot be handled by a single robot end-effector thereby enhancing their working volume and grasping capability.

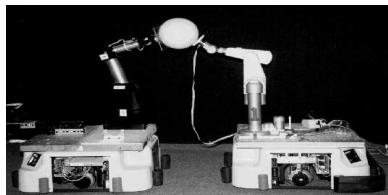


Figure 1: A team of two cooperating mobile manipulators marching while grasping an object

In our experimental testbed shown in Figure 1, two mobile manipulators are used to cooperatively grasp

*This work was in part supported by: BCS 92-16691, MSS-91-57156, CISE/CDA 88-22719, ARPA Grant N00014-92-J-1647 and Army Grant DAAH04-96-1-0007

and transport an object. Each mobile manipulator consists of a robot arm mounted on a TRC Labmate platform. The platform is a nonholonomic cart with two actuated degrees-of-freedom. The mobile platforms enable appropriate (and even optimal) positioning and configuring before grasping, and possible reconfiguration if necessary. Some interesting maneuvers which may be necessary for obstacle avoidance are shown in Figures 2, 3, and 4. In this way they can follow the desired trajectory for the object while reconfiguring rather than having to stop, retract and change their formation.

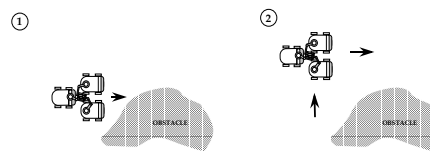


Figure 2: Executing a “parallel-parking” maneuver to circumvent an obstacle

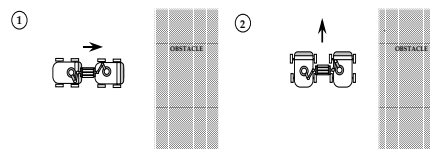


Figure 3: Making a sharp turn when confronted with a wall. The agents reconfigure from a single file formation to a “march abreast” formation.

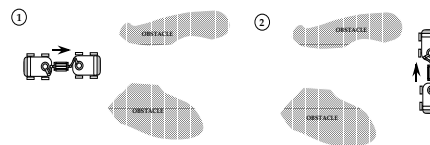


Figure 4: Reconfiguring from a “single file” formation to a “single file” formation while maneuvering through a corridor

Each agent is equipped with force/torque sensors and can sense the actions of the other agent. During

a cooperative manipulation task, the only information that is exchanged at servo rates is force information [1]. In a typical maneuver, each agent is given a nominal trajectory for the object. Each platform follows an appropriate trajectory while the manipulators maintain a stable grasp.

In recent years many researchers have investigated control of nonholonomic systems. A car or a car with trailers are typical examples of such systems. Brockett [2] showed that no smooth state-feedback control law can asymptotically stabilize a nonholonomic system to a specified configuration even if the system is controllable. However stabilization can be achieved using non-smooth feedback laws [3, 4], smooth time-varying feedback laws [5] or non-smooth, time-varying schemes [6]. There is an important class of nonholonomic systems that can be converted to a canonical form also known as a chained form [3, 7, 8]. In these papers and in [9] different open-loop strategies have been proposed to steer chained systems to a desired configuration. The conversion into the chained form requires tedious analytical manipulations. It is also not clear how paths avoiding obstacles can be obtained. However, very few results are available for the synthesis of open-loop controls.

The generation of optimal trajectories for nonholonomic systems has been addressed in [10]. A fundamental result for car-like systems was derived by Reeds and Shepp [11]. Building on the work of Dubins [12] they have showed that minimum-distance trajectories for a car are composed of circular arcs and straight lines. Using this result, Laumond et al. [13] have proposed an efficient algorithm for planning near minimum distance trajectories for a car moving among obstacles. Fernandes et al. [14] use optimal control methods to find trajectories that minimize the L_2 norm of the input vector. They use Ritz' method to approximate the solution with a small number of basis functions. Such approaches do not work very well when state constraints are imposed on the system since optimal inputs can become discontinuous. If an optimal trajectory to a desired trajectory is known, there are methods (see, for example, [15, 16]) to efficiently control the system along the desired trajectory.

In this paper, we focus on the problem of planning maneuvers such as the ones shown in Figures 2, 3, and 4. We will mainly focus on the task of determining the optimal trajectory for two reasons. The platform controllers in our experimental system only allow velocity control. Secondly, the methods for determining optimal actuator torques in the presence of unilateral constraints are addressed elsewhere [17] and the extension to the case where dynamics are incorporated is straight forward.

We first consider the formulation of the optimal control problem for our system of mobile manipula-

tors. The numerical approach is summarized in Section 3. The optimal control problem for this specific system is presented in Section 4 and in Section 5, numerical solutions are computed. The experimental results are presented in Section 6 and concluding remarks are made in Section 7.

2 Optimal control

Consider a dynamic system described by state equations

$$\dot{x} = f(x(t), u(t), t). \quad (1)$$

The vector x denotes the state of the system while u is the input vector. The state of the system is known at some initial time t_0 and is prescribed for some, possibly unknown, time t_f . The cost functional is

$$J = \int_{t_0}^{t_f} L(x(t), u(t), t) dt \quad (2)$$

and the controls are restricted to a set U . The problem of optimal control is to find a piecewise smooth input vector $u \in U$ that brings the system from a known initial state x_0 to a desired final state x_f so that the cost functional J is minimized.

Suppose that the set of admissible controls, U , is defined by a set of equalities

$$g_i(x, u, t) = 0 \quad i = 1, \dots, k \quad (3)$$

and a set of inequalities

$$h_i(x, u, t) \leq 0 \quad i = 1, \dots, l. \quad (4)$$

Each inequality constraint can be converted to an equality constraint

$$h_i(x, u, t) \leq 0 \Leftrightarrow \hat{h}_i = h_i(x, u, t) + \xi_i^2 = 0 \quad (5)$$

where ξ_i is an (unconstrained) slack variable. Next, define a Hamiltonian

$$H = L(x, u, t) + \lambda^T (\dot{x} - f(x, u, t)) + \phi^T g + \psi^T \hat{h}. \quad (6)$$

Note that the constraints g and h have been adjoined to the Hamiltonian with vectors of multipliers ϕ and ψ . Now define an extended state vector

$$X = [X_x^T, X_\mu^T, X_\lambda^T, X_\phi^T, X_\psi^T, X_\xi^T]^T \quad (7)$$

where the individual components are defined by

$$\begin{aligned} X_x &= x, & \dot{X}_\mu &= u, & \dot{X}_\lambda &= \lambda, \\ \dot{X}_\phi &= \phi, & \dot{X}_\psi &= \psi, & \dot{X}_\xi &= \xi. \end{aligned} \quad (8)$$

Consider the following variational problem:

$$\min J(X) = \int_{t_0}^{t_f} H(t, X, \dot{X}) dt. \quad (9)$$

where the boundary conditions are given by

$$\begin{aligned} X_x(t_0) &= x_0, & X_x(t_f) &= x_f, & X_\mu(t_0) &= 0, \\ X_\lambda(t_0) &= 0, & X_\phi(t_0) &= 0, & X_\psi(t_0) &= 0, \\ X_\xi(t_0) &= 0. \end{aligned} \quad (10)$$

It can be shown that the critical solutions of the unconstrained variational problem (9) are exactly the extremals for the optimal control problem (1-4) obtained from the Minimum Principle [18, page 109].

3 Numerical method

Consider a general variational calculus problem:

$$\min \int_{t_0}^{t_f} H(t, X, \dot{X}) dt \quad (11)$$

subject to the boundary conditions on X at t_0 and t_f . Define an admissible variation $z(t)$ to be a piecewise smooth function that satisfies the boundary conditions at t_0 and t_f . It can be shown that if $X(t)$ is a solution of the variational problem (11), then the integral equation

$$\int_{t_0}^{t_f} [F_X^T z + F_{\dot{X}}^T \dot{z}] dt = 0 \quad (12)$$

holds for all admissible variations $z(t)$. Here F_X and $F_{\dot{X}}$ denote partial derivatives with respect to X and \dot{X} respectively.

To numerically compute a critical solution, we first discretize the interval $[t_0, t_f]$ so that $t_0 = a_0 < a_1 < \dots < a_N = t_f$. For simplicity, we will assume that $a_i - a_{i-1} = h$ for $i = 1, \dots, N$. Then we introduce a set of piecewise linear shape functions

$$\alpha_k(t) = \begin{cases} \frac{t - a_{k-1}}{h} & \text{if } a_{k-1} < t \leq a_k, \\ \frac{a_{k+1} - t}{h} & \text{if } a_k < t \leq a_{k+1}, \\ 0 & \text{otherwise, } (k = 0, \dots, N). \end{cases} \quad (13)$$

The variation $z(t)$ is piecewise smooth, so each of its components can be approximated with a sum $\hat{z}_i = \sum_{j=0}^N z_{ij} \alpha_j(t)$. Using the central difference scheme to approximate the derivatives and the mean-value theorem to approximate the integral (12) on each subinterval $[a_{i-1}, a_i]$, the following set of vector equations in the unknown values Z_k at points $k = 1, \dots, N-1$ is obtained:

$$\begin{aligned} 0 = & \frac{h}{2} F_X \left(\frac{a_k + a_{k-1}}{2}, \frac{X_k + X_{k-1}}{2}, \frac{X_k - X_{k-1}}{h} \right) + \\ & F_{\dot{X}} \left(\frac{a_k + a_{k-1}}{2}, \frac{X_k + X_{k-1}}{2}, \frac{X_k - X_{k-1}}{h} \right) + \\ & \frac{h}{2} F_X \left(\frac{a_{k+1} + a_k}{2}, \frac{X_{k+1} + X_k}{2}, \frac{X_{k+1} - X_k}{h} \right) - \\ & F_{\dot{X}} \left(\frac{a_{k+1} + a_k}{2}, \frac{X_{k+1} + X_k}{2}, \frac{X_{k+1} - X_k}{h} \right) \quad (14) \end{aligned}$$

Note that unknowns Z_k are vectors. In all, we have $n(N+1)$ unknowns. We also have $n(N-1)$ equations (14). The remaining $2n$ equations are obtained from the boundary conditions, if they exist, or from the transversality conditions. These are of the similar form as equations (14) and the reader should consult [18] for detailed derivations.

The resulting system of nonlinear equations is solved using the Newton-Raphson method. Each equation only depends on the three adjacent points. The matrix of the system of linear equations solved during the iteration is thus block-tridiagonal and the system can be solved very efficiently.

4 Motion planning for two cooperating agents

We consider the system of two cooperating agents shown in Figure 1. The manipulators are nonredundant. The main task is to find the trajectories which connect the desired initial and final configurations of each platform and the object, while ensuring that the two manipulators can cooperatively grasp the object. Thus, it is sufficient, in this problem, to consider a kinematic model for the system.

Each platform is a nonholonomic cart with the state equations:

$$\begin{aligned} \dot{x}_1 &= u_1 \cos \theta_1 & \dot{x}_2 &= u_3 \cos \theta_2 \\ \dot{y}_1 &= u_1 \sin \theta_1 & \dot{y}_2 &= u_3 \sin \theta_2 \\ \dot{\theta}_1 &= u_2 & \dot{\theta}_2 &= u_4 \end{aligned} \quad (15)$$

where (x_i, y_i) is the position of the reference point and θ_i is the orientation of the i th ($i = 1, 2$) cart. The nonholonomic constraint restricts the velocity of the cart so that the linear velocity of the reference point is parallel to the longitudinal axis of the vehicle. The inputs u_1 and u_3 are the linear velocities of the reference points and u_2 and u_4 the angular velocities of the respective platforms.

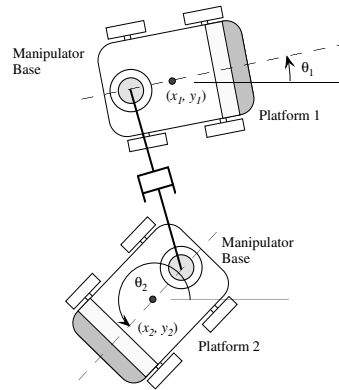


Figure 5: Theoretical model

We do not explicitly model the kinematics of the manipulators as we are not interested in the planning of motion of each manipulator. Instead we imagine the bases of the manipulators being connected by a planar $R-P-R$ kinematic chain as shown in Figure 5. The revolute joints coincide with the base joints. The distance between the two revolute joints is denoted by l . The prismatic joint between the two revolute joints has limited range of motion. In this way it is ensured that the mobile platforms do not drift too far apart or come too close. These limits on l model the limited reach of the manipulators and the need to keep the object in the dextrous workspace of each manipulator. The $R-P-R$ chain does not restrict

the maneuverability of a platform relative to the other unless the prismatic joint is at a joint limit. The joint limit is modeled by unilateral constraints on the state:

$$l_{lower} \leq l \leq l_{upper} \quad (16)$$

In addition, we impose a constraint on the turning radius or the steering angle ¹. It can be written in the form:

$$\rho_{min1}^2 u_2^2 - u_1^2 \leq 0 \quad \rho_{min2}^2 u_4^2 - u_3^2 \leq 0 \quad (17)$$

Here ρ_{min1} (ρ_{min2}) is the minimum radius of curvature for the path of the reference point on cart 1 (cart 2).

We now treat the variational problem of determining the shortest path connecting two given positions and orientations subject to the above constraints. The distance is measured in terms of the arc lengths traversed by the drive wheels of the two carts. Minimization of distance is mathematically equivalent to minimization of the integral of the square of the velocities. Thus we obtain the following cost function:

$$\min \frac{1}{2} \int_{t_0}^{t_f} \{(u_1^2 + u_3^2) + B^2(u_2^2 + u_4^2)\} dt$$

where B is a scaling factor that depends on the geometry of the vehicle.

To reduce this problem to the form in (11) we define the state vector:

$$x = [x_1, y_1, \theta_1, x_2, y_2, \theta_2]^T$$

and the extended state vector as :

$$X = [x^T, X_\mu^T, X_\lambda^T, X_\psi^T, X_\xi^T]^T \quad (18)$$

where

$$\begin{aligned} \dot{X}_\mu &= [u_1 \ u_2 \ u_3 \ u_4]^T & \dot{X}_\psi &= [\psi_1 \dots \psi_4]^T \\ \dot{X}_\lambda &= [\lambda_1 \dots \lambda_6]^T & \dot{X}_\xi &= [\xi_1 \dots \xi_4]^T \end{aligned}$$

The inequalities can be converted to equalities and written in the following form :

$$\begin{aligned} \hat{h}_1 &= \rho_{min1}^2 u_2^2 - u_1^2 + \xi_1^2 \\ \hat{h}_2 &= \rho_{min2}^2 u_4^2 - u_3^2 + \xi_2^2 \\ \hat{h}_3 &= l_{lower} - l + \xi_3^2 \\ \hat{h}_4 &= l - l_{upper} + \xi_4^2 \end{aligned} \quad (19)$$

At this point the Hamiltonian for the variational problem can be formulated.

The final variational problem has 24 unknowns. Some of them also have to satisfy boundary conditions. Given a starting (x_0) and final (x_f) position and orientation for the two platforms, the boundary conditions are:

$$\begin{aligned} x(t_0) &= x_0, & x(t_f) &= x_f, & X_\mu(t_0) &= 0, \\ X_\lambda(t_0) &= 0, & X_\psi(t_0) &= 0, & X_\xi(t_0) &= 0. \end{aligned} \quad (20)$$

¹In our example (see Section 6), because the two drive wheels have a common axle, the platforms can turn without translating and this constraint is not required. But in a more general system, this is not possible and the turning radius will be limited).

5 Simulation Results

In the numerical simulations and experiments that follow, we used the parameters from our experimental testbed shown in Figure 1 and described in Section 6. These parameters are: $\rho_{min1} = \rho_{min2} = 0.1m$, $B = 0.3m$, $l_{lower} = 0.9m$ and $l_{upper} = 1.1m$. We chose a total of 161 mesh points for our simulation and required a relative accuracy of 10^{-7} in our state variables for convergence.

Figures 6-8 show optimal motion plans for the maneuvers shown in Figures 2 - 4. The initial position and orientation for all the examples is given by $x_0 = [0, 0, 0, -1, 0, 0]^T$.

Figure 6.a and 6.b display the path of reference points and motions of the two platforms during a ‘‘parallel parking’’ maneuver. The object is moved laterally through a 1 meter distance. The arcs in the platform trajectories at the beginning and towards the end of the maneuver turn out to have the same minimal turning radius as predicted by [11] for a single platform.

In Figure 7.a and 7.b, the path of the reference point and motions of the two platforms is shown for a 90 degree turn without moving the object significantly (see Figure 3). Similarly, an example of the reconfiguring maneuver is shown in Figure 8.

The required linear and angular velocities of the two platforms during the parallel parking maneuver are shown in Figure 9. The step changes in linear velocity correspond to points at which the trajectories of two reference points cease to be circular.

The generation of optimal trajectories for the examples shown here with a mesh size of 150 points

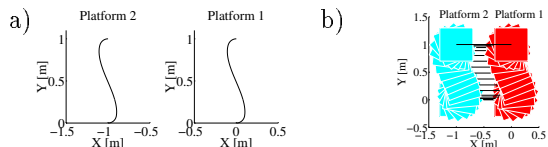


Figure 6: Paths (a) and motions (b) for parallel parking maneuver.

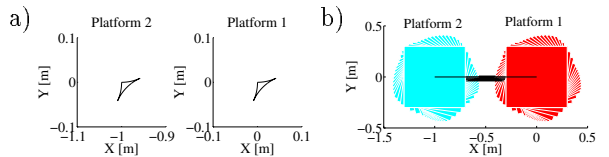


Figure 7: Paths (a) and motions (b) for a 90° turn.

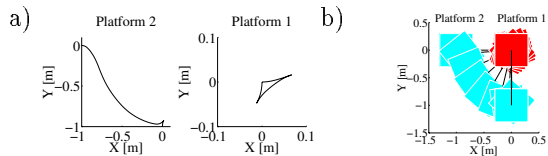


Figure 8: Paths (a) and motions (b) for a reconfiguration maneuver. (note that the plots are on different scales.)

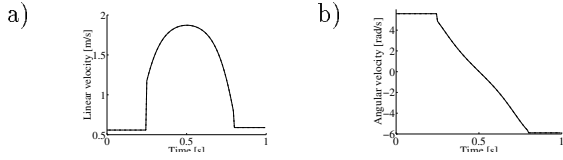


Figure 9: Velocities (a) and Angular velocities (b) for a parallel parking maneuver (identical for both platforms).

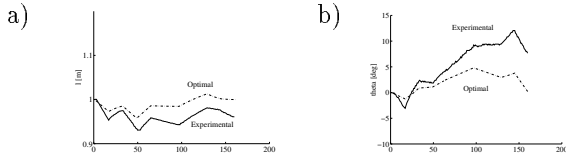


Figure 10: Variation of distance (a) and relative angle between platforms (b), $\theta_2 - \theta_1$, for a 90° turn.

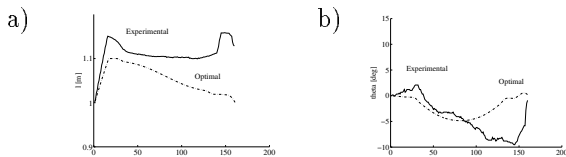


Figure 11: Variation of distance (a) and relative angle between platforms (b), $\theta_2 - \theta_1$, for a parallel parking maneuver.

takes approximately 10 seconds on a Sparc 10 station. Crude solutions with fewer mesh points can be obtained faster. For example, a grid size of 10 yields a solution in 4 seconds.

6 Experiments

The experimental testbed consists of two mobile manipulators. The TRC platforms are computer controlled nonholonomic vehicles which have two DC-motor actuated wheels with encoders and four casters, one at each corner. The linear and angular velocities of the drive wheels can be controlled through a RS-232 serial line at bandwidth of 15Hz. Each platform is controlled by an IBM 386 PC compatible computer. The wheel rotations are used in a dead-reckoning scheme to estimate the position and orientation of the platform for real time control. The relative position and orientation between the two platforms is measured through an instrumented four-bar-linkage. Each joint of this linkage is equipped with an encoder, but this information is only used for analyzing the performance of the system; it is not used for real-time control. Finally we should point out that there is currently no way of experimentally measuring the absolute position and orientation of the two platforms.

In the experiments, the platforms are commanded to follow the planned trajectories while the manipulators are commanded to maintain a stable grasp. The platform control is based on position feedback that is obtained from dead-reckoning. Therefore the com-

manded position (and velocity) trajectories are translated into position (and velocity) trajectories for the drive wheels, and the wheels are appropriately controlled based on position feedback using proportional control.

We show the experimental results in Figures 10-11. In all these plots the variation of the relative position and orientation (measured by the instrumented four bar linkage) is shown and compared with the relative position and orientation computed from the optimal motion plan. The results for the 90° turn maneuver are shown in Figure 10. We compare the variation in l (the distance between the bases of the two manipulators) and $\theta = \theta_2 - \theta_1$ (the relative angle between the two platforms) for the optimal motion plan and the experiment. Ideally we would like to see no discrepancy between the two sets of plots. However, because the platform control is accomplished with dead-reckoning [19], we can see that the experimental trajectory drifts from the commanded trajectory with time. The angular discrepancy between the commanded (optimal) and the experimental trajectory is as much as 7 degrees.

In Figure 11, we show the same results for the parallel parking maneuver. The errors due to dead-reckoning are seen to be more pronounced especially if we look at the variation of l with time. Here the optimal motion plan requires l to be at its upper limit (1.1 meters). The experimental results show that l overshoots the optimal trajectory and therefore violates this constraint. Obviously, this can be circumvented if the optimal path is generated with a factor of safety on the constraints (e.g., with the limits on l between 0.95 and 1.05 meters). More importantly, it is clear that such an open loop approach to control may not be satisfactory for the types of maneuvers we are interested in.

The errors in dead-reckoning mainly occur when there are reversals in the paths of any of the drive motors or the passive wheels (casters in our case). The reversal of a drive motor invariably results in slip while the reversal of the path of castor causes it to change its configuration (the center of the spherical ball of the castor will always trail the pin along which the vertical load is transmitted) which in turn results in frictional forces that indirectly cause the drive wheels to slip. In an experiment where we commanded a platform to go forward and backward on a 1 meter straight line track, the angular errors were observed to be 3 degrees per meter. This is consistent with the discrepancy between the experimental and the optimal trajectories in the plots.

7 Concluding remarks

We considered a system of two mobile manipulators (agents) for cooperative manipulation and material handling, and the motion planning problem for such a system. We presented a general method to generate optimal trajectories for the agents for any given maneuver. The formulation allows easy inclusion of additional constraints such as limits on the turning radii or limits on the distance between the mobile platforms. We presented numerical solutions for some typical maneuvers, such as changing formation, abrupt turns and parallel parking in cluttered environments. Experiments were conducted in which the planned trajectories were used as reference inputs and the performance of a simple control scheme based on dead-reckoning was evaluated.

An important direction for future work is incorporating obstacles into the optimal control planning algorithm using distance functions [20, 21]. A distance function returns a numerical value that is a measure of how far a point in configuration space is from a collision. This is easily included in the Hamiltonian with appropriate slack variables.

It is important to develop a control scheme that will use information about the relative position and orientation between the platforms with the information obtained through dead-reckoning to improve the performance. The information about the relative position and orientation can be obtained through additional sensors (e.g., acoustic). However, it may be simpler to use the joint sensors on the manipulators on each platform to compute this information. This is also a subject for future research.

References

- [1] R. Bajcsy, V. Kumar, M. Mintz, R. Paul, and X. Yun, "Cooperative agents: Machines and humans," in *Proceedings of the 1993 International Conference on Automation and Robotics*, (Tokyo, Japan), Nov 1-4 1993.
- [2] R. W. Brockett, "Asymptotic stability and feedback stabilization," in *Differential Geometric Control theory* (R. W. Brockett, R. S. Millman, and H. J. Sussman, eds.), pp. 181-191, Boston: Birkhauser, 1983.
- [3] O. Egeland, E. Berglund, and O. J. Sordalen, "Exponential stabilization of a nonholonomic underwater vehicle with constant desired configuration," in *Proc. of 1994 IEEE Int. Conf. on Robotics and Automation*, (San Diego, CA), pp. 20-25, May 1994.
- [4] A. M. Bloch, M. Reyhanoglu, and N. H. McClamroch, "Control and stabilization of nonholonomic dynamic systems," *IEEE Transactions on Automatic Control*, vol. 37, no. 11, pp. 1746-1756, 1992.
- [5] C. Samson, "Time-varying feedback stabilization of car-like wheeled mobile robots," *The International journal of robotics research*, vol. 12, no. 1, pp. 55-64, 1993.
- [6] C. C. de Wit and O. J. Sordalen, "Exponential stabilization of mobile robots with nonholonomic constraints," *IEEE Transactions on Automatic Control*, vol. 37, no. 11, pp. 1791-1797, 1992.
- [7] R. M. Murray and S. S. Sastry, "Nonholonomic motion planning: steering using sinusoids," *IEEE Transactions on Automatic Control*, vol. 38, no. 5, pp. 700-716, 1993.
- [8] D. Tilbury, R. M. Murray, and S. S. Sastry, "Trajectory generation for the n -trailer problem using Goursat normal form," *IEEE Transactions on Automatic Control*, vol. 40, no. 5, pp. 802-819, 1995.
- [9] L. G. Bushnell, D. M. Tilbury, and S. S. Sastry, "Steering three-input nonholonomic systems: the fire truck example," *The International Journal of Robotics Research*, vol. 14, no. 4, pp. 366-381, 1995.
- [10] J.-C. Latombe, *Robot motion planning*. Boston: Kluwer Academic Publishers, 1991.
- [11] J. A. Reeds and L. A. Shepp, "Optimal paths for a car that goes both forwards and backwards," *Pacific. J. of Math.*, vol. 145, no. 2, pp. 367-393, 1990.
- [12] L. E. Dubins, "On curves of minimal length with a constraint on average curvature and with prescribed initial and terminal positions and tangents," *American Journal of Mathematics*, vol. 79, pp. 497-516, 1957.
- [13] J.-P. Laumond, P. E. Jacobs, M. Taix, and R. M. Murray, "A motion planner for nonholonomic mobile robots," *IEEE Transactions on Robotics and Automation*, vol. 10, no. 5, pp. 577-593, 1994.
- [14] C. Fernandes, L. Gurvits, and Z. X. Li, "Optimal motion planning for a falling cat," tech. rep., Courant Institute of Mathematical Sciences, New York, May 1991. Robotics Research Laboratory.
- [15] C. Samson and K. Ait-Abderrahim, "Feedback control of a nonholonomic wheeled cart in Cartesian space," in *Proc. of 1991 International Conference on Robotics and Automation*, (Sacramento, CA), pp. 1136-1140, Apr. 1991.
- [16] G. Walsh, D. Tilbury, S. Sastry, R. Murray, and J. P. Laumond, "Stabilization of trajectories for systems with nonholonomic constraints," *IEEE Transactions on Automatic Control*, vol. 39, no. 1, pp. 216-222, 1994.
- [17] M. Žefran and V. Kumar, "Optimal control of systems with unilateral constraints," in *Proc. of 1995 IEEE Int. Conf. on Robotics and Automation*, (Nagoya, Japan), 1995.
- [18] J. Gregory and C. Lin, *Constrained optimization in the calculus of variations and optimal control theory*. New York: Van Nostrand Reinhold, 1992.
- [19] J. Borenstein and Y. Koren, "Motion control analysis of a mobile robot," *ASME Journal of Dynamic systems, Measurement, and Control*, vol. 109, pp. 73-79, June 1987.
- [20] E. G. Gilbert, D. W. Johnson, and S. S. Keerthi, "A fast procedure for computing the distance between complex objects in three-dimensional space," *IEEE Journal of Robotics and Automation*, vol. 4, no. 2, pp. 193-203, 1988.
- [21] M. C. Lin and J. F. Canny, "A fast algorithm for incremental distance calculation," in *Proceedings of 1991 International Conference on Robotics and Automation*, (Sacramento, CA), pp. 1008-1014, Apr. 1991.